THERMAL SHOCK RESISTANCE AND MECHANICAL CHARACTERISTICS OF MATERIALS BASED ON ZIRCONIUM DIOXIDE

A. G. Gashchenko, G. A. Gogotsi, A. G. Karaulov, and I. N. Rudak

UDC 539.4

Ceramics based on zirconium dioxide are being more widely used in various branches of high-temperature technology due to their high refractoriness.

It has been established that to obtain ceramic parts with a high thermal shock resistance a microcrazed structure must be obtained, which can be formed in zirconium dioxide due to the formation of two phases in the material – cubic and monoclinic. In this case the amount of monoclinic (unstabilized) phase in zirconium dioxide stabilized, for example, with calcium oxide should be 20-40% [1]. The microcrazed structure in this case is evidently formed due to the high microstresses that occur at monoclinic-cubic phase boundaries at the phase transformation temperature during firing of the part. These microstresses may reach 28,000 kg/cm^2 [2]. The number of stressed zones and, consequently, the number and length of microcracks in the material are determined by the degree of stabilization, i.e., the quantity and size of inclusions of monoclinic phase in the basic material.

This work concerns the effect of the degree of stabilization of materials based on zirconium dioxide on their thermomechanical properties. We investigated commercial zirconium dioxide stabilized with 4, 6, and 8 mole % yttrium oxide with holding at 1750°C for 18 h. Monoclinic ZrO_2 was added to zirconium dioxide stabilized with 6 and 8 mole % Y_2O_3 in order to regulate the phase composition within wide limits. The mixture was fired at 1750°C for 6 h. The charge for preparation of the samples consisted of a granular mass with different grain sizes – 50% 1-0.5 mm, 10% 0.5-0.8 mm, and 40% less than 0.088 mm.

The samples were compacted under a pressure of 1000 kg/cm^2. The composition and properties after firing are given in Table 1; the structure is shown in Fig. 1.

The thermal shock resistance of the materials was determined experimentally by creating a temperature differential in the wall of hollow cylindrical samples. The tests were made in the TS-4 apparatus with a PRT-1 temperature regulator, with additional measurements of radial movements and tensometric measurements on the outer surface [3]. Cylindrical samples with the following dimensions were used: o.d. 75 mm, i.d. 25 mm, h 12.5 mm. The thermal loading rate was constant – 200 deg/min. On samples with these dimensions and at this heating rate the inner surface fractured before any noticeable increase in temperature on the outer surface, which ensured operation of the measuring instruments without substantial errors in temperature.

The circumferential deformation of each sample was recorded by means of four 2PKB-10 strain gages symmetrically arranged on the outer surface of the sample. A characteristic strain diagram for 6TM samples is shown in Fig. 2, where the "delayed" fracture of this composition under the influence of thermal stresses can be seen. The first drop of the strain occurs in the region of strain gages II and III which is due to the formation of an initial crack similar to that observed previously [4]. The sharp decline of the deformation during further thermal stress was recorded simultaneously by all strain gages at the time the crack passed through the entire wall of the samples. For this reason, the parameters taken as characteristic of the thermal shock resistance were as follows: $\Delta T'$ is the temperature differential corresponding to the beginning of nonsteady movement of the crack, °C; $\Delta T''$ is the increase of the

Institute of Strength Problems, Academy of Sciences of the Ukrainian SSR, Kiev. Ukrainian Institute of Refractory Materials, Khar'kov. Translated from Problemy Prochnosti, No. 6, pp. 76-80, June, 1974. Original article submitted July 3, 1973.

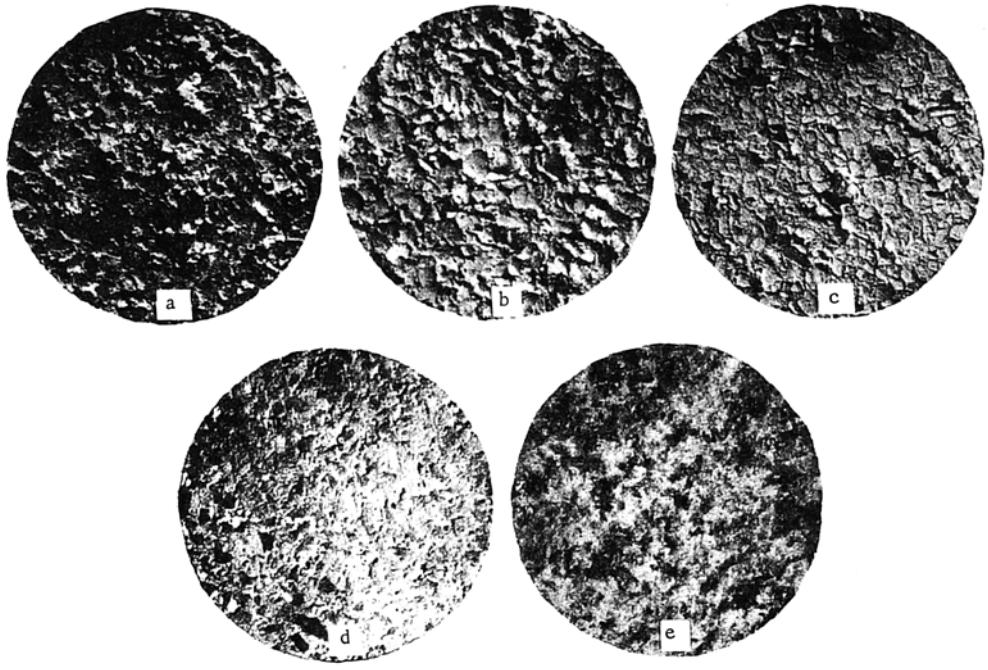

Fig. 1. Structure of materials investigated: a) 6TM; b) 8TM; c) 4T; d) 6T; e) 8T. Light microscope (×10). Reduced 2/3 in reproduction.

TABLE 1*

Material	Composition of samples, %		Phase composition (monoclinic phase), %
	ZrO_2	Y_2O_3	
4T	89,2	8,0	30
6T	88	10,2	10
8T	84	14,0	—
6TM	90,2	7,1	52
8TM	86,1	11,2	32

*Data from Ukrainian Scientific- Research Institute of Refractory Materials (UNIIO).

temperature differential causing development of the thermal crack through the entire thickness of the wall of the hollow cylindrical sample, °C; ΔT is the breaking temperature differential recorded at the time the thermal crack passes completely through the wall of the sample; $\Delta T = \Delta T' + \Delta T''$.

The results of determining the thermal shock resistance are given in Table 2, where it can be seen that "delayed" failure occurs only in samples of incompletely stabilized ZrO_2. Figure 3 shows the change in the breaking temperature differential in relation to the degree of stabilization of the material, i.e., the extent of microcrazing. It follows from Fig. 3 that the higher thermal shock resistance of material based on ZrO_2 is due mainly to the resistance to propagation of thermal cracks, since an increase of the monoclinic component up to 50% affects only the breaking temperature differential of ZrO_2.

It is evident that to determine the thermal shock resistance of this type of material one must use a criterion of thermal shock resistance describing the behavior of the material before the initial thermal crack occurs $R = \sigma_t(1-\mu)/E\alpha$, and the energy criterion $R^N = \gamma_{eff}E/\sigma_t^2(1-\mu)$ taking into account the resistance of refractory materials to crack propagation. Thus, the first must correspond to the temperature differential $\Delta T'$, and the energy criterion to $\Delta T''$. In calculating the capacity of materials to resist crack propagation we used the characteristics of fracture toughness. In conformity with [5], the effective surface energy of failure is

$$\gamma_{eff} = \frac{G_c}{2}, \tag{1}$$

where G_c is the fracture toughness determined on reaching the critical conditions of loading of samples with a crack.

Since the following relationship exists between the characteristics of fracture toughness:

$$G_{1c} = \frac{K_{c1}}{E(1-\mu^2)}, \tag{2}$$

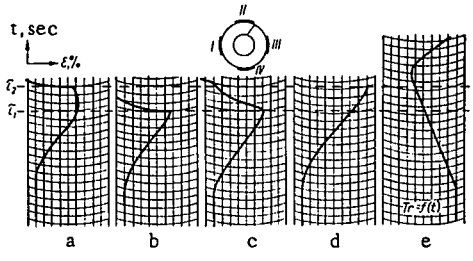

Fig. 2

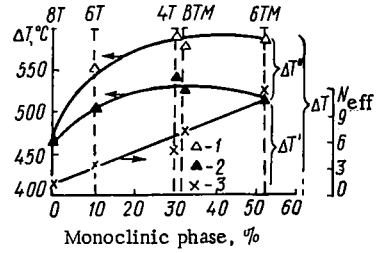

Fig. 3

Fig. 2. Characteristic strain diagram of the outer surface of 6TM samples during thermal loading: a-d) strain gages I-IV and their readings; e) reading of thermocouple on the inner surface of the sample [τ_1) time corresponding to the beginning of nonsteady thermal crack propagation; τ_2) time the thermal crack passes completely through the wall of the sample].

Fig. 3. Variation of the breaking temperature differentials ΔT, ΔT', and the number of thermal cycles to failure N with the degree of stabilization of the material: 1) ΔT; 2) ΔT'; 3) N.

TABLE 2

Material	$\Delta T'$, °C	$\Delta T''$, °C	ΔT, °C	R, deg	T_c, cm	N, cycles
4T	546	49	595	176	0,67	5
6T	506	48	554	154	0,39	3
8T	465	0	465	118	0,17	1
6TM	527	65	592	174	1,13	11
8TM	530	53	583	122	1,0	7

the energy criterion of thermal shock resistance R^{IV} can be written in the form

$$R^{IV} = \frac{K_{Ic}^2}{2\sigma_t^2 (1-\mu^2)(1-\mu)}. \quad (3)$$

For most refractory materials the value of μ varies within limits of 0.25-0.35. Neglecting it in the case of comparative calculations based on criteria calculated by formula (3) thus leads to an error of ~6%. Thus, the energy criterion of thermal shock resistance can be written in simplified form

$$T_c = \frac{K_{Ic}}{\sigma_t}. \quad (4)$$

The correlation of the breaking temperature differential ΔT' and the computed values of criterion R, and also ΔT" with the energy criterion T_c, can be seen from Fig. 4. It was of interest, as previously, to check the experimental results of thermal shock resistance tests by analytical calculations with use of the energy criterion under conditions of thermal impact loading. Thermal impact tests were made by the method generally used, by heating 30 × 30 mm samples in a Kryptol furnace to 1600°C and cooling in running water (temperature 20°C). These tests results are given in Table 2, and the correlation between them and the data from analytical calculations by the energy criterion can be seen in Fig. 4b. Thus, differential application of the thermal shock resistance criterion shows satisfactory agreement between the experimental and analytical values.

The mechanical characteristics of all compositions were determined by three-point bending of prismatic samples 100 × 15 × 10 mm on an RM-101 machine equipped with a reversing gear and an electric furnace [7]. The results were treated in accordance with concepts of the linear-elastic behavior of materials.

To determine the tendency of the materials to crack formation we determined the critical stress intensity factor K_{Ic}.

The tests were made with prismatic samples with a lateral crack, for which purpose two lateral cuts were made at an angle of 120° from each other (Fig. 5a), with initiation of the crack by a blow at the bottom of the cut (Fig. 5b). A deformation diagram in coordinates of bending versus force was made during tests under conditions of three-point bending. The load corresponding to the beginning of nonsteady movement of the initial crack was determined at the point where the diagram deviates from a linear relationship. The length of the initial crack before the tests was measured by means of the MG-1 microscope. The value of K_{Ic} was calculated by the equation [8]:

TABLE 3

Material	σ_{bend}, kg/cm²			$E \cdot 10^{-5}$, kg/cm²			K_{Ic}, kg/cm$^{-3/2}$ at 20°C	l_c, cm, at 20°C	$\alpha \cdot 10^{-5}$, deg^{-1}		
	20° C	400° C	800° C	20° C	400° C	800° C			20° C	400° C	800° C
4T	71,0	95,0	205,0	0,807	0,555	0,49	48	0,16	0,5	0,5	0
6T	84,0	70,0	67,8	0,655	0,888	0,46	32	0,046	0,8	1,17	1,17
8T	285,0	177,0	157,0	3,07	2,55	1,68	48	0,0088	0,8	1,17	1,17
6TM	45,1	33,6	63,0	0,52	0,354	0,32	51,5	0,44	0,5	0,6	0,75
8TM	43,1	42,0	51,9	0,503	0,328	0,38	43,3	0,32	0,7	0,7	0,62

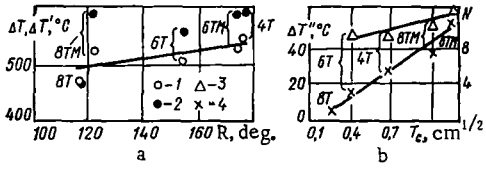

Fig. 4

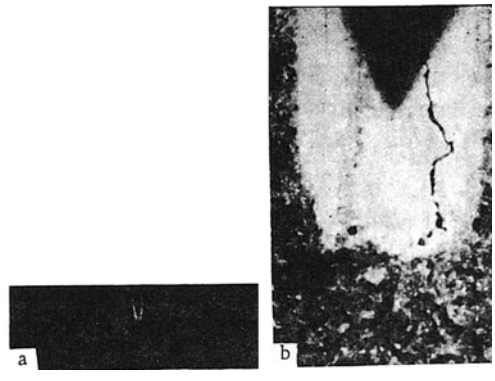

Fig. 5

Fig. 4. Comparison of experimental results of thermal shock resistance tests with analytical values: 1) $\Delta T'$; 2) ΔT; 3) $\Delta T''$; 4) N.

Fig. 5. Sample for ductile fracture test with saw cut (a) and crack initiated at the bottom of the cut before the test (b).

$$K_{Ic} = Y\frac{6Ma^{1/2}}{bh^2}, \tag{5}$$

where M is the bending moment; a is the length of the initial crack; b is the width of the sample; h is the height of the sample; Y is a function of the size of the original crack in the sample.

The results of determining the physicomechanical characteristics are given in Table 3.

From the values of K_{Ic} we found the critical crack length (Table 3) [5]:

$$l_k = \frac{K_{Ic}^2}{1.12\pi\sigma_{bend}}. \tag{6}$$

It can be seen from comparing the data in Fig. 1 and Table 3 that the results of mechanical tests can to some extent determine quantitatively the increase in the degree of microcrazing of the material with increasing amounts of monoclinic phase. It is characteristic that with increasing amounts of monoclinic phase the critical length of the initial microcrack increases. In this case the mechanical strength and the modulus of elasticity decrease (Fig. 6).

From the relationship shown in Fig. 6 it can be seen that even with a small amount of monoclinic phase in material based on ZrO_2 the strength decreases considerably.

From the values of σ_{bend} and l_c we plotted (logarithmic coordinates) $\log\sigma_{bend} = f(\log 1/l_c)$ (Fig. 7). The satisfactory grouping of the experimental points close to a straight line and the slope of the line to the x axis at an angle α for which $\tan\alpha = 1/2$ indicate the correspondence of the experimental relationships to the well-known equation

$$\sigma = Al^{-1/2}, \tag{7}$$

where A is an empirical constant of the material; l_c is the critical crack length.

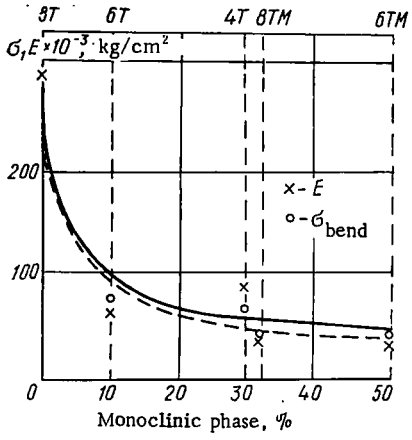

Fig. 6.

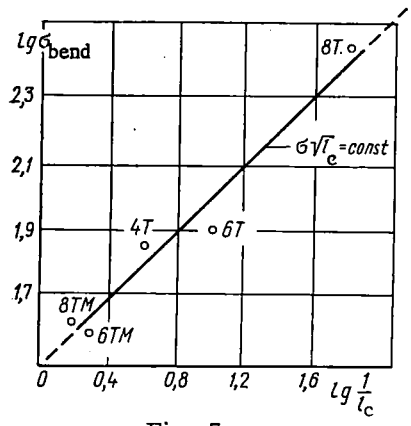

Fig. 7

Fig. 6. Variation of bending strength and Young's modulus with degree of stabilization of the material.

Fig. 7. $\mathrm{Log}\,\sigma_{\mathrm{bend}} = f(\log 1/l_c)$.

There are similar changes in strength with variation of the grain size, which is described by the equation [7]

$$\sigma = Ad^{-1/2}.$$

An increase in the length of the original microcrack with increasing amounts of the monoclinic component can also be seen in structural examinations of the material (Fig. 1).

LITERATURE CITED

1. A. G. Karaulov et al., Izv. Akad. Nauk SSSR, Neorg. Mater., 3, 6 (1967).
2. A. G. King and P. I. Jaworsky, J. Amer. Cer. Soc., No. 1 (1968).
3. G. A. Gogotsi, A. G. Gashchenko, and A. A. Kurashevskii, Probl. Prochnosti, No. 4 (1972).
4. G. A. Gogotsi, A. G. Gashchenko, et al., Ogneupory, No. 1 (1973).
5. B. A. Drozdovskii (editor), Applied Problems of Fracture Toughness [Russian translation], Mir, Moscow (1968).
6. D. P. H. Hasselman, J. Amer. Cer. Soc., No. 8 (1969).
7. A. G. Gashchenko et al., Probl. Prochnosti, No. 4 (1973).
8. W. F. Brown and J. E. Srawley, Plane Strain Crack Toughness Testing of High Strength Metallic Materials, ASTM, Philadelphia (1966).